The Astrophysical Journal, 772:19 (11pp), 2013 July 20 doi:10.1088/0004-637X/772/1/19

ON THE LIRA LAW AND THE NATURE OF EXTINCTION TOWARD TYPE Ia SUPERNOVAE

Francisco Förster[1,2], Santiago González-Gaitán[1], Gastón Folatelli[3], and Nidia Morrell[4]
[1] Departamento de Astronomía, Universidad de Chile, Casilla 36-D, Santiago, Chile
[2] Center for Mathematical Modelling, Universidad de Chile, Avenida Blanco Encalada 2120 Piso 7, Santiago, Chile
[3] Kavli Institute for the Physics and Mathematics of the Universe, Todai Institutes for Advanced Study (TODIAS), University of Tokyo, 5-1-5 Kashiwanoha, Kashiwa, Chiba 277-8583, Japan
[4] Las Campanas Observatory, Carnegie Observatories, Casilla 601, La Serena, Chile
Received 2012 November 28; accepted 2013 April 23; published 2013 July 2

ABSTRACT

We have studied the relation between the color evolution of Type Ia supernovae (SNe Ia) from maximum light to the *Lira law* regime and the presence of narrow absorption features. Based on a nearby sample of 89 SNe Ia, we have found that the rate of change of $B-V$ colors at late phases (between 35 and 80 days after maximum) varies significantly among different SNe Ia. At maximum light, faster Lira law $B-V$ decliners have significantly higher equivalent widths of blended Na I D1 and D2 narrow absorption lines, redder colors, and lower R_V reddening laws. We do not find faster Lira law $B-V$ decliners to have a strong preference for younger galaxy environments, where higher interstellar material (ISM) column densities would be expected. We interpret these results as evidence for the presence of circumstellar material. The differences in colors and reddening laws found at maximum light are also present 55 days afterward, but unlike the colors at maximum they show a significant variation among different host galaxy morphological types. This suggests that the effect of ISM on the colors is more apparent at late times. Finally, we discuss how the transversal expansion of the ejecta in an inhomogeneous ISM could mimic some of these findings.

Key words: distance scale – supernovae: general

Online-only material: color figures

1. INTRODUCTION

Type Ia supernovae (SNe Ia) are thought to be the thermonuclear explosion of white dwarf stars. They are one of the main sources of iron in the universe (e.g., Matteucci & Greggio 1986) and are key tools for cosmological distance determinations (Phillips 1993; Hamuy et al. 1996), leading to the discovery of the acceleration of the universe (Riess et al. 1998; Perlmutter et al. 1999). Despite much observational and theoretical effort, we lack a clear understanding about their progenitors (for reviews, see Hillebrandt & Niemeyer 2000; Wang & Han 2012).

Most favored progenitor scenarios involve a carbon–oxygen white dwarf (CO WD) in a binary system. The CO WD could either ignite at the Chandrasekhar mass after accreting matter stably from a companion in a delayed detonation or pure deflagration explosion (Chandrasekhar mass–single degenerate scenario; Hachisu et al. 1996, 1999a, 1999b; Li & van den Heuvel 1997; Langer et al. 2000; Han & Podsiadlowski 2004; Meng et al. 2009; Wang et al. 2009; Khokhlov 1991; Röpke & Niemeyer 2007; Kromer et al. 2013; Nomoto et al. 1984; Röpke et al. 2012), at a mass below the Chandrasekhar mass if accretion is unstable and a surface detonation is strong enough to trigger a central detonation (sub-Chandrasekhar mass–single degenerate scenario; Nomoto 1982; Woosley et al. 1986; Sim et al. 2010; Kromer et al. 2010), or after the merger with a degenerate companion in a double degenerate scenario if the detonation can occur in a dynamical timescale (violent double degenerate merger, violent DD; Iben & Tutukov 1984; Webbink 1984; Pakmor et al. 2012; Röpke et al. 2012). Some observational tests for these scenarios are (1) the presence or absence of low velocity circumstellar material (CSM) left from the accretion process or from previous nova explosions, (2) the presence or absence of a companion star, (3) the SN rate delay-time distribution, which is generally found to be inversely proportional to the time since formation (for a review, see Maoz & Mannucci 2012) and is generally believed to favor DD scenarios (although see Kobayashi & Nomoto 2009), and (4) the degree of neutronization in the central regions due to different central densities at ignition (e.g., Gerardy et al. 2007).

Although the lack of evidence for shocked companion stars of the progenitor CO WDs, shocked pre-supernova winds, or companion pre-explosion images is more generally consistent with DD scenarios (Li et al. 2011; Nugent et al. 2011; Bloom et al. 2012; Brown et al. 2012; Schaefer & Pagnotta 2012; Edwards et al. 2012), there are different results that suggest the presence of CSM around SN Ia progenitors, which is generally expected in single degenerate scenarios (or slow DD mergers; see Fryer et al. 2010). These consist of optical colors that favor scattering in nearby material (Wang 2005; Goobar 2008; Amanullah & Goobar 2011), and narrow absorption lines that show variability (Patat et al. 2007; Blondin et al. 2009; Simon et al. 2009), are blueshifted (Sternberg et al. 2011; Foley et al. 2012), or that correlate with certain SN ejecta viewing angles (Förster et al. 2012). This evidence is in contrast to the absence of X-ray or radio emission from shocked CSM in the nearby SN 2011fe (Horesh et al. 2012), but is supported by recent observations of SN Ia PTF11kx (Dilday et al. 2012), which was probably surrounded by narrow nova shells ejected before explosion, and the sample of SNe Ia with CSM interaction recently identified by Silverman et al. (2013).

If some SNe Ia are surrounded by significant amounts of CSM, then it would be expected that the light from those SNe would be scattered away from the line of sight by intervening dust, causing extinction and reddening, but also that it would be scattered into the line of sight by nearby dust, i.e., multiple scattering processes or light echoes (e.g., Chevalier 1986; Wang 2005; Patat 2005; Patat et al. 2006; Goobar 2008). The typical delay of these light echoes would depend on the typical

distance to the closest surviving dust after explosion, which for typical distances of about 0.005–0.1 pc (see, e.g., Patat et al. 2007; Simon et al. 2009) would correspond to approximately 6–112 days of light travel-time. Assuming that the light echoes and/or dust sublimation at later times change the SN light curves at these timescales after maximum,[5] we have performed a systematic study of the evolution of late time colors of SN Ia during the Lira law regime (Lira 1995; Phillips et al. 1999), between 35 and 80 days after maximum. Given that SN colors evolve in an approximately homogeneous fashion during this phase, we try to detect the presence of multiple scattering processes, or light echoes, studying the evolution of colors in a big sample of nearby SNe Ia and its relation with the presence of narrow absorption features.

In order to distinguish between interstellar material (ISM) and CSM, we have studied the relation between the equivalent widths (EWs) of blended Na I D1 and D2 narrow absorption features, obtained from mid-resolution spectra using the method described in Förster et al. (2012, hereafter FG12) with the Lira law $B-V$ decline rates. Extinction by ISM should in principle only shift the $B-V$ colors to higher values, without significant changes of the Lira law $B-V$ decline rate, whereas CSM can both shift the $B-V$ colors to higher values and change the Lira law $B-V$ decline rate, making it generally faster as the distance to the CSM is reduced (Amanullah & Goobar 2011) or if CSM dust is destroyed at late times. Given that systems with significant CSM should have a different extinction law (Wang 2005; Goobar 2008), we also study the relation between $B-V$ and $V-i$ colors at maximum and 55 days after maximum for different Lira law $B-V$ decline rates in our sample. To discard that SN light curves have different intrinsic decline rates for different galaxy populations, we have also performed several environmental tests studying the distributions of host galaxy morphological type, host galaxy inclination, stretch, or Δm_{15} of different Lira law $B-V$ decline rates.

Energy deposition during the Lira law regime is dominated by the β-decay of ^{56}Co into ^{56}Fe, via electron captures (81%) or positron emissions (19%). At 35 days after maximum, energy deposition is dominated by the scattering of γ-rays produced in the primary channel. At 80 days after maximum, the ejecta becomes transparent to γ-rays and the kinetic energy from positrons produced in the secondary channel dominates the energy deposition (Milne et al. 1999). This means that a transition from γ-ray to positron energy deposition occurs during the Lira law regime, which may be linked to different bolometric decline rates. However, to our knowledge, there is not a clear connection between the bolometric decline rate with the $B-V$ decline rates observed during the Lira law.

Finally, given the connection found by FG12 between narrow absorption features and the nebular velocity shifts introduced by Maeda et al. (2010), interpreted as evidence for CSM in positive nebular velocity shift SNe Ia and a general asymmetry of the CSM post-explosion, we have tested whether there is any correlation between nebular velocity shifts and the observed Lira law $B-V$ decline rates.

2. SAMPLE SELECTION AND ANALYSIS

We have selected those SNe Ia that have spectra in the Center for Astrophysics (CfA) public sample of SNe Ia (Blondin et al. 2012) or in the Carnegie Supernova Program (CSP) sample of nearby SNe Ia (Folatelli et al. 2013). For every spectrum of every SN we have run an automatic Python script to measure EWs and associated errors of blended Na I D1 and D2 narrow absorption features as described in FG12. These values were combined using a weighted average to obtain one EW and associated error per SN, assigning an EW of zero to those SNe with negative measurements. We then selected those SNe with final EW errors below 0.6 Å.

For the photometry, we used data from CfA3 and CfA4 (Hicken et al. 2009, 2012), CSP (Contreras et al. 2010; Stritzinger et al. 2010, 2011), and other sources (see Table 1). When multiple sources were available, we used either only CSP or only CfA data depending on the numbers of photometric points available. We corrected for Milky Way extinction using the maps of Schlegel et al. (1998) and performed K corrections and S corrections to the natural rest-frame system of the Las Campanas Observatory (LCO; Stritzinger et al. 2011) using photometry-adjusted spectral template series from Hsiao et al. (2007). In those cases where the natural system of the instrument is not provided and the photometry is only given in the system of Landolt (1992), we transform from there to the LCO system. We selected only those SNe Ia with good photometric coverage during the Lira law regime (between 35 and 80 days after maximum), which we defined as those SNe having at least three simultaneous B and V photometric data points with a minimum separation of 25 days between the first and last observations.

For the final sample, we fitted a linear relation in the $B-V$ versus time plane between 35 and 80 days after maximum. This led to two values and associated errors for every SNe Ia: the $B-V$ color at 55 days and the Lira law $B-V$ decline rate. We retained only those SNe Ia that had an error associated with the Lira law $B-V$ decline rate smaller than 0.006 mag day^{-1}.

For every SN in the sample we also fitted stretch and colors at maximum using SiFTO (Conley et al. 2008), requiring at least one data point between −15 and 7.5 days after B-band maximum and another one between 2.5 and 35 days after B-band maximum in each band, as well as Δm_{15} values and $E(B-V)$ extinction values using SNooPY (Burns et al. 2011). For most purposes, stretch and Δm_{15} are equivalent quantities describing the light curve shape diversity of SNe Ia, but we use both to account for systematic effects in our analysis. We also obtained inclinations and host galaxy morphological types using the Asiago catalog (Barbon et al. 1999) when available. In order to discard the effects introduced by possibly very different populations in the SN Ia sample, we have also removed sub-luminous SNe Ia, which we define as those SNe Ia whose stretch is smaller than 0.7 and whose $B-V$ color at maximum is higher than 0.4.

In Figure 1(a), the $B-V$ color evolution for selected SNe is shown and in Figure 1(b) for the entire sample used in this analysis, separated by the Lira law $B-V$ decline rate. Figure 1(a) hints that different Lira law $B-V$ decline rates occur among different SNe Ia (see also Wang et al. 2008b). In the following, we explore whether or not the Lira law $B-V$ decline rate is related to other observational characteristics in the sample.

3. RESULTS

3.1. Lira Law $B-V$ Decline Rates versus Equivalent Widths and Colors

In Figure 2, we show the EWs of blended narrow Na I D1 and D2 absorption features versus the Lira law $B-V$ decline rate according to the sample defined in Section 2. From the figure it is clear that the distribution of EWs of those SNe with faster

[5] We define maximum as the maximum of the SN light curve in the B band.

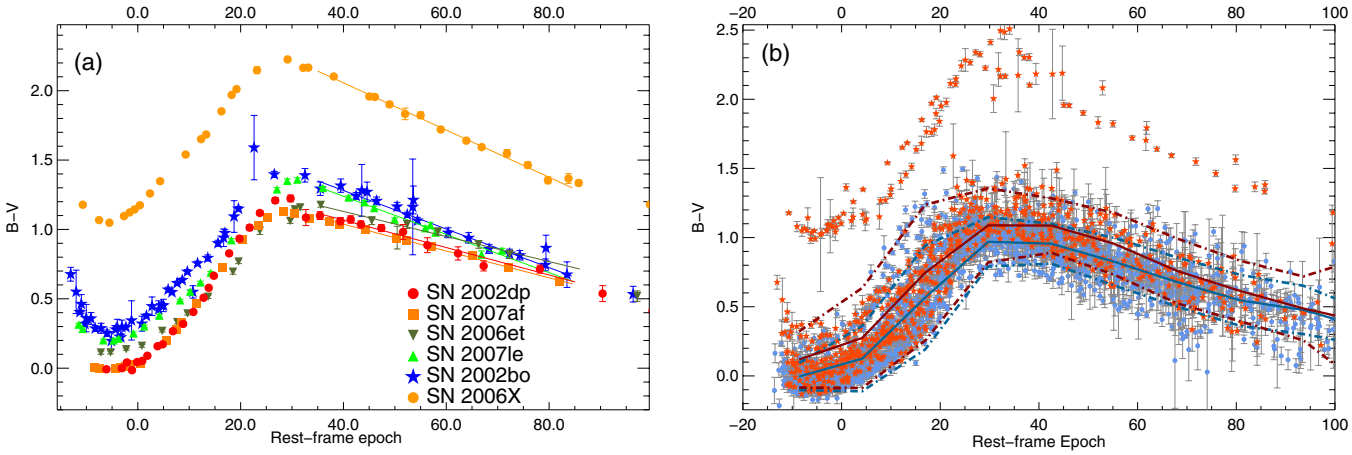

Figure 1. (a) $B-V$ evolution for selected SNe and (b) for the entire sample defined in Section 2, dividing the sample between SNe with the Lira law $B-V$ decline rates faster (red stars) and slower (blue dots) than -0.013 mag day^{-1}. We plot the median evolution and observed dispersion for each sample with red and blue lines, respectively. It can be seen that faster Lira law $B-V$ decliners are redder at maximum and 55 days afterward.

(A color version of this figure is available in the online journal.)

Table 1
Nearby SNe Ia Used in This Analysis Besides Data from the Center for Astrophysics (CfA3 and CfA4: Hicken et al. 2009, 2012) and the Carnegie Supernova Program (CSP: Contreras et al. 2010; Stritzinger et al. 2010)

Name	Source
SN 1993ae	Riess et al. (1999)
SN 1994D	Meikle et al. (1996); Altavilla et al. (2004)
SN 1994ae	Riess et al. (2005); Altavilla et al. (2004)
SN 1995D	Riess et al. (1999); Sadakane et al. (1996)
SN 1995al	Riess et al. (1999)
SN 1995bd	Riess et al. (1999); Altavilla et al. (2004)
SN 1996C	Riess et al. (1999)
SN 1997E	Jha et al. (2006)
SN 1997cw	Jha et al. (2006)
SN 1998ab	Jha et al. (2006)
SN 1998aq	Riess et al. (2005)
SN 1998bp	Jha et al. (2006)
SN 1998dm	Jha et al. (2006); Ganeshalingam et al. (2010)
SN 1998dh	Jha et al. (2006); Ganeshalingam et al. (2010)
SN 1998ef	Jha et al. (2006); Ganeshalingam et al. (2010)
SN 1998es	Jha et al. (2006)
SN 1999aa	Krisciunas et al. (2000); Altavilla et al. (2004); Jha et al. (2006)
SN 1999ac	Jha et al. (2006); Phillips et al. (2006)
SN 1999gd	Jha et al. (2006)
SN 1999gh	Jha et al. (2006); Ganeshalingam et al. (2010)
SN 1999dq	Jha et al. (2006)
SN 1999gp	Jha et al. (2006); Ganeshalingam et al. (2010); Krisciunas et al. (2001)
SN 2000B	Jha et al. (2006)
SN 2000cx	Candia et al. (2003); Altavilla et al. (2004); Sollerman et al. (2004); Jha et al. (2006)
SN 2000dk	Jha et al. (2006); Ganeshalingam et al. (2010)
SN 2000fa	Jha et al. (2006); Ganeshalingam et al. (2010)
SN 2002aw	Ganeshalingam et al. (2010)
SN 2002bo	Krisciunas et al. (2004); Benetti et al. (2004); Ganeshalingam et al. (2010)
SN 2002cs	Ganeshalingam et al. (2010)
SN 2002dl	Ganeshalingam et al. (2010)
SN 2003cg	Elias-Rosa et al. (2006); Ganeshalingam et al. (2010)
SN 2003du	Anupama et al. (2005); Stanishev et al. (2007); Leonard et al. (2005)
SN 2004bg	Ganeshalingam et al. (2010)
SN 2004bk	Ganeshalingam et al. (2010)

Note. Note that we do not include data from the YALO telescope because of possible inconsistencies with its photometric system (Krisciunas et al. 2003; Phillips et al. 2006).

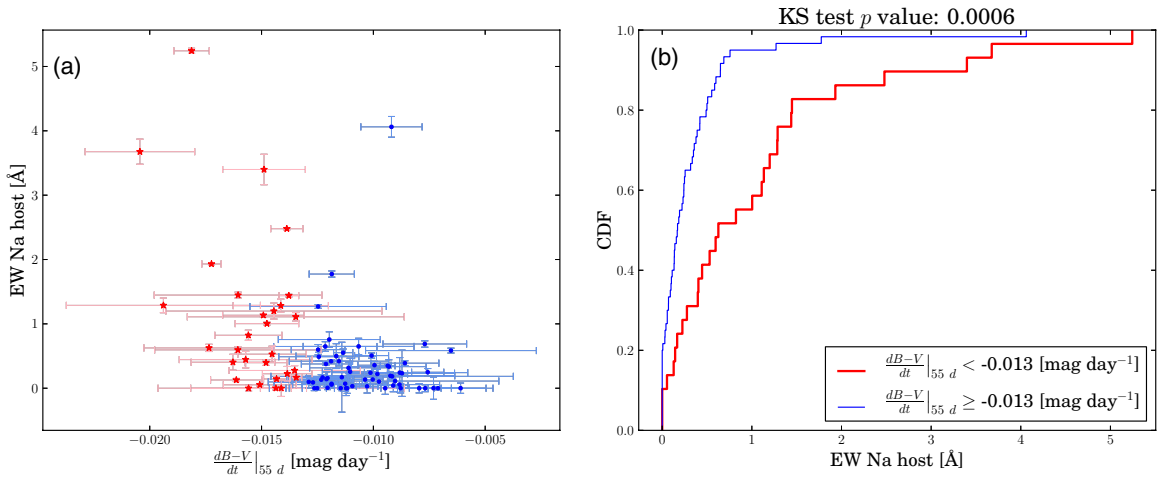

Figure 2. (a) Equivalent widths of narrow Na I D1 and D2 blended absorption features vs. the Lira law $B-V$ decline rate for fast (red stars) and slow (blue dots) Lira law $B-V$ decliners and (b) the corresponding Kolmogorov–Smirnov (K-S) test for the cumulative distribution of equivalent widths of narrow Na I D1 and D2 blended absorption features for fast (red) and slow (blue) Lira law $B-V$ decline rates for the sample defined in Section 2. The division between fast and slow Lira law $B-V$ decliners is defined to be at -0.013 mag day^{-1} (see Section 3.4).

(A color version of this figure is available in the online journal.)

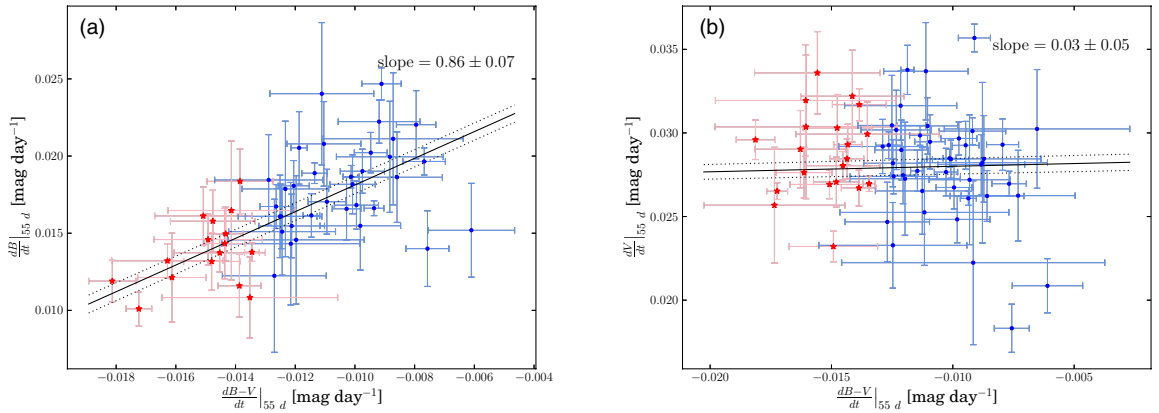

Figure 3. (a) Lira law B-band decline rates vs. Lira law $B-V$ decline rates for fast (red stars) and slow (blue dots) Lira law $B-V$ decliners and (b) Lira law V-band decline rates vs. Lira law $B-V$ decline rates for fast (red stars) and slow (blue dots) Lira law $B-V$ decliners. We found that the diversity of $B-V$ decline rates is mostly due to different B-band decline rates during the Lira law, and not to V-band decline rate variations, suggesting that the origin of the diversity has a larger effect at shorter wavelengths.

(A color version of this figure is available in the online journal.)

Lira law $B-V$ decline rates is different from that of SNe Ia with slower $B-V$ decline rates. If we divide the sample by a Lira law $B-V$ decline rate of -0.013 mag day^{-1}, then we determine with a Kolmogorov–Smirnov (K-S) test that there is a probability of 0.0006 that the resulting distributions of EWs arise from the same parent population. This division of the sample is based on finding the Lira law $B-V$ decline rate that maximizes the differences between fast and slow Lira law $B-V$ decliners (explained in more detail in Section 3.4) and it implies that 33% of the SNe in the sample are defined as fast Lira law $B-V$ decliners.

In order to study the effect of positron absorption, we investigate whether the differences between fast and slow $B-V$ Lira law decliners are related to their bolometric decline rates during the Lira law, which we approximate by their V-band decline rates (see, e.g., Cappellaro et al. 1997). We found that fast and slow Lira law $B-V$ decliners do not have significantly different distributions of V-band decline rates, with a K-S test probability of 0.86 that their distributions of V-band decline rates arise from the same parent population. However, we find a significant difference between their distributions of B-band decline rates, with a K-S test probability of only 0.0001 that their distributions of B-band decline rates arise from the same parent population. Thus, the Lira law $B-V$ decline rate diversity is driven primarily by different B-band decline rates, in the direction that fast Lira law $B-V$ decliners are slow Lira law B decliners.[6] The fact that the Lira law $B-V$ decline rate is connected to the presence of narrow absorption features suggests that this effect is either caused by younger progenitor systems having slower Lira law B decline rates, which would be associated with star forming regions and larger gas/dust column densities, or to the presence of CSM that causes the B-band evolution to become slower at late times. We show the B- and V-band decline rates versus the $B-V$ decline rates in Figure 3.

If faster Lira law $B-V$ decliners are associated with more material in the line of sight, then we should also expect a difference in the distributions of colors around maximum light of fast and slow Lira decliners. In fact, the distributions of

[6] Note that this is different from the B-band decline rate directly after maximum, which is connected to different stretch or Δm_{15} values.

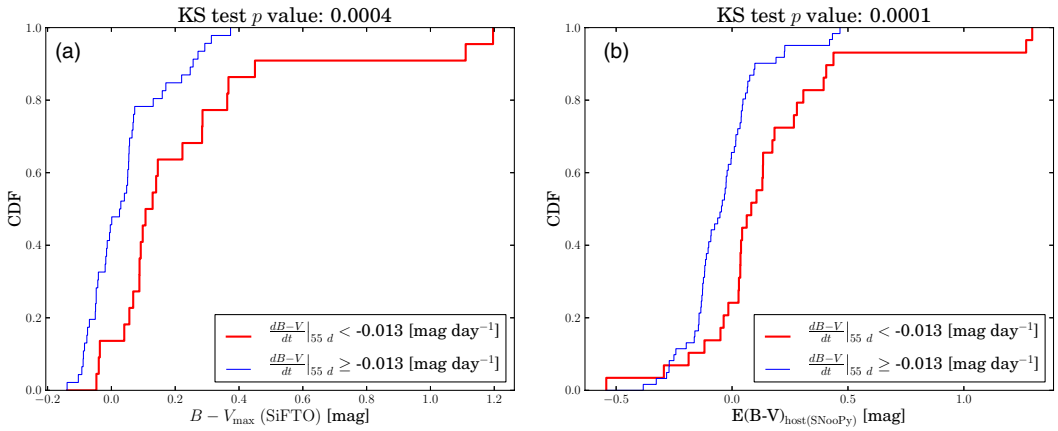

Figure 4. (a) K-S tests for the distributions of $B-V$ colors at maximum obtained from SiFTO dividing the sample by the Lira law $B-V$ decline rate and (b) K-S tests for the distributions of $E(B-V)$ extinction values obtained from SNooPY dividing the sample by the Lira law $B-V$ decline rate. Fast Lira law $B-V$ decliners are redder at maximum, have stronger Na I D1 and D2 absorption, but have no strong preference for any particular environment (see Section 3.2), which is consistent with them having more CSM.

(A color version of this figure is available in the online journal.)

Table 2
K-S Test for the Distribution of Observed Properties Dividing the Sample by Lira Law $B-V$ Decline Rates

K-S Test	EW(Na)	$B-V$ at Max.	$E(B-V)$	$B-V$ at 55 Days
p value	0.0006	0.0004	0.0001	0.003

Notes. The null hypothesis is that fast and slow Lira law $B-V$ declining SNe Ia have the same distribution of blended Na I D1 and D2 narrow absorption features, colors at maximum (SiFTO), extinction values (SNooPY), or colors 55 days after maximum.

Table 3
K-S Test for the Distribution of Observables Dividing the Sample by Lira Law $B-V$ Decline Rates

K-S Test	Host Morph. Type	Host. Incl.	Stretch	Δm_{15}
p value	0.10	0.19	0.18	0.07

Notes. The null hypothesis is that fast and slow declining Lira law SNe Ia have the same distribution of host morphological types, host inclinations, stretch, or Δm_{15}. The null hypothesis cannot be discarded in any of these tests, suggesting that the equivalent width and color differences seen in Figure 2 are not driven by environmental factors.

$B-V$ colors at maximum obtained with SiFTO and $E(B-V)$ extinctions obtained from SNooPY are significantly different if we divide the sample between fast and slow Lira law $B-V$ decliners with p values of 0.0004 and 0.0001, respectively. This is shown in Figure 4. Fast and slow Lira law $B-V$ decliners also differ significantly in their colors 55 days after maximum (p value of 0.003). It should be noted that fast and slow Lira law $B-V$ decliners tend to have more similar colors at late times during the Lira law, as redder SNe in $B-V$ tend to decrease faster in $B-V$. These results are summarized in Table 2.

3.2. Environmental and SN Intrinsic Effects

After finding that differences in the measured Lira law $B-V$ decline rates are related to the presence of material in the line of sight, we tested whether this could be explained by faster Lira law $B-V$ decliners occurring in younger stellar environments, i.e., whether the material detected could be ISM. In order to do this, we divide our sample by quantities that should favor higher ISM column densities, such as host galaxy morphological type or host galaxy inclinations (removing E/S0s from the sample, where it is difficult to define an inclination). If there was a strong preference for morphological type among different Lira law $B-V$ decline rates, then it could mean that younger systems decay faster during the Lira law and that there is no need to invoke CSM as an explanation. If there was a strong preference for galaxy inclination, then it would suggest that the Lira law $B-V$ decline rate is affected by ISM in the line of sight.

Stretch and Δm_{15} are also thought to be associated with the age of the progenitor systems (Hamuy et al. 1995, 1996; Riess et al. 1999; Hamuy et al. 2000; Sullivan et al. 2006), which we also confirmed in our sample, with p values of less than 0.00001 for the null hypothesis that the distributions of stretch and Δm_{15} dividing the sample between earlier- and later-type hosts arise from the same parent population. Thus, stretch and Δm_{15} play a role similar to the host galaxy morphological type in the sense that younger systems (larger stretch or smaller Δm_{15}) occur in regions where the ISM column density should be larger. Therefore, if stretch or Δm_{15} were connected to the evolution of $B-V$ at late times, then it could suggest that environment could drive the different Lira law $B-V$ decline rates. On the other hand, stretch and Δm_{15} are known to account for most of the diversity of SN Ia light curves because they are likely related to the enclosed mass of ^{56}Ni or iron group elements in the ejecta, which is the power source of SN Ia light curves. Considering that at late times the physics of the decay of ^{56}Co and the absorption of positrons start to become more relevant, it is not unreasonable to think that both stretch and Δm_{15} could be related to the Lira law $B-V$ decline rate.

Thus, we test whether the distributions of host morphological type, host inclination, stretch, and Δm_{15} of fast and slow Lira law $B-V$ decliners arise from the same parent population. In none of the tests did we obtain strongly significant differences (see Table 3). Therefore, assuming that the Lira law $B-V$ decline rate is not strongly affected by the amount of ISM in the line of sight, we interpret the results shown in Table 2 as evidence for CSM around those SNe Ia having the fastest Lira law $B-V$ decline rates (but see Section 3.6).

The presence of CSM could easily change the slope of the Lira law $B-V$ decline rate, either by multiple scattering processes (i.e., CSM light echoes; see Amanullah & Goobar 2011) or

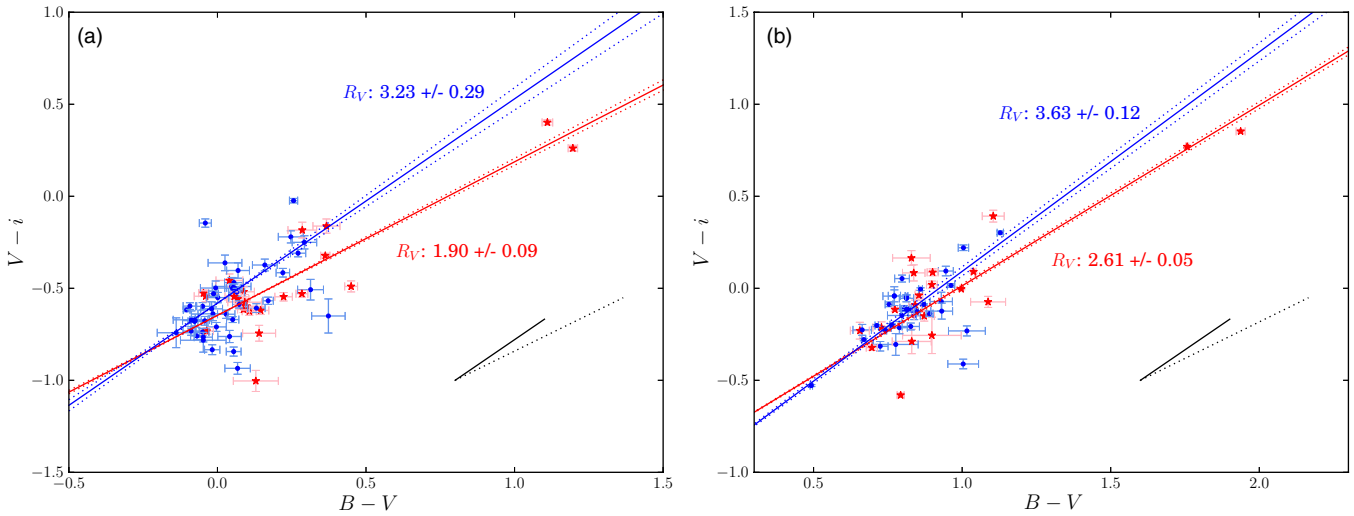

Figure 5. (a) $V-i$ and $B-V$ color at maximum light and (b) 55 days after maximum light, dividing the sample between fast (red stars) and slow (blue dots) Lira law $B-V$ decliners. We fit a straight line to the $V-i$ vs. $B-V$ colors at maximum light and 55 days after maximum for each sample. At maximum light and 55 days after maximum, the extinction laws are significantly different, with significantly lower R_V for fast Lira law $B-V$ decliners at all times, although becoming more similar to slow Lira law $B-V$ decliners 55 days after maximum light. We show for reference extinction vectors with $A_V = 1$ for $R_V = 3.2$ (continuous) and $R_V = 1.7$ (dashed). If we remove the highest extinction SNe from the fast declining sample, then we obtain an even lower R_V at maximum.

(A color version of this figure is available in the online journal.)

Table 4
K-S Test for the Distribution of $B-V$ Colors at Maximum ($B-V_{\rm max}$) and 55 Days after Maximum ($B-V_{55}$), Dividing the Sample by Lira Law $B-V$ Decline Rates (Columns 1 and 2) or by the Median Morphological Type (Columns 3 and 4)

K-S Test	$B-V_{\rm max}$	$B-V_{55}$	$B-V_{\rm max}$	$B-V_{55}$
Sample division	Lira law $B-V$ decline rate		Morphological type	
p value	0.0004	0.003	0.16	0.003

Notes. The null hypothesis is that fast and slow Lira law $B-V$ declining SNe Ia have the same distribution of colors at maximum light and 55 days after maximum light, or that earlier- and later-type hosts have the same distribution of colors at maximum and 55 days after maximum light. These results suggest that the reddening effect of CSM is more apparent at early times and that of ISM at late times.

by the progressive destruction of nearby dust if the material is sufficiently close to the expanding ejecta, making the $B-V$ colors increasingly bluer at late times and, as a consequence, the Lira law $B-V$ decline rates faster. This was also noted by Folatelli et al. (2010) in systems with color excesses that were moderate to large.

If the $B-V$ colors at maximum are mainly driven by CSM reddening and if either light echoes or late time CSM dust destruction occur, then we would expect that the reddening observed during maximum light should decrease at later times, making the reddening first be dominated by CSM and later by ISM. In fact, we cannot rule out that the distributions of colors at maximum in the earlier- and later-type hosts—or lower and higher inclination hosts—arise from the same parent population (p values of 0.16 and 0.39, respectively), as was also found in previous studies (see, e.g., Johansson et al. 2013, cf. Sullivan et al. 2010). This would be expected if the colors of SN Ia at maximum were primarily driven by ISM. However, we do rule out that the distributions of colors 55 days after maximum in earlier- and later-type hosts arise from the same parent population (p value of 0.003). This suggests that (1) $B-V$ colors at maximum and 55 days after maximum are driven by different physical effects, and (2) $B-V$ colors 55 days after maximum are more related to the properties of the environment where SNe occur. This is consistent with the CSM interpretation presented above when the Lira law decline rates are considered. These results are summarized in Table 4.

We should emphasize that we are not suggesting that ISM absorption is irrelevant at maximum light, but only that it does not drive the results shown in Table 2 (although see Section 3.6). In fact, we detect a highly significant increase on the EWs of Na I D1 and D2 due to ISM-related properties by performing K-S tests on the distribution of EWs of Na I D1 and D2 dividing a bigger sample by host galaxy type, host galaxy inclination, stretch, or Δm_{15} instead of by Lira law $B-V$ decline rate, with p values smaller than 0.00001 in all cases.

3.3. $V-i$ Colors and Dust Reddening Laws (R_V)

A prediction from Goobar (2008) is that those SNe Ia with more CSM should have a steeper reddening law toward the blue. Thus, we expect that fast Lira law $B-V$ decliners should have a lower R_V at maximum light if CSM was present in these systems, which can be measured using $V-i$ colors. In Figure 5, we show the $V-i$ versus $B-V$ colors at maximum and 55 days after maximum with best-fitting R_V values assuming the reddening law of Cardelli et al. (1989) and O'Donnell (1994). To estimate the R_V best-fitting errors, we have performed a Monte Carlo analysis based on the measured B, V, and i magnitudes and their errors. We created 1000 realizations of these magnitudes at maximum and 55 days after maximum to derive $B-V$ and $V-i$ colors, which by definition are correlated, and then derive 1000 best-fitting R_V values, whose standard deviation was used as the error.

We find that fast Lira law decliners have a steeper reddening law (lower R_V) than slow Lira law decliners, a result that becomes more pronounced at maximum light, even after removing the highly reddened SN 2003cg and SN 2006X. In fact, the R_V values that best match the data for fast and slow Lira law decliners are $R_V = 1.90 \pm 0.09$ and $R_V = 3.23 \pm 0.29$,

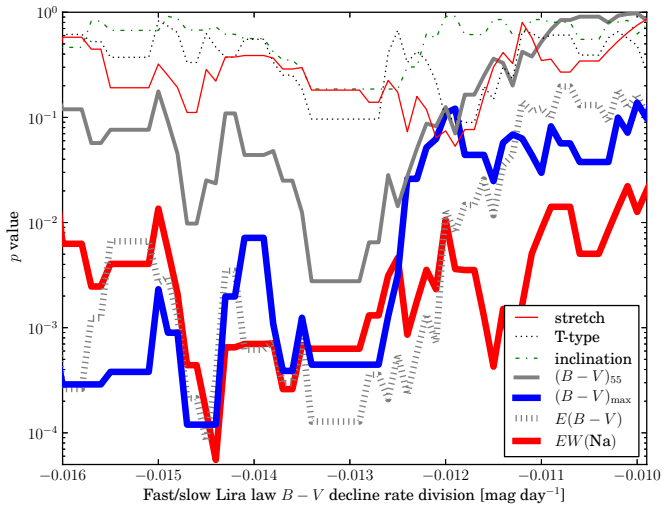

Figure 6. K-S test p values for the null hypothesis that the distribution of the variables indicated by the labels arise from the same parent population when dividing the sample by the Lira law $B-V$ decline rate shown in the x-axis. This plot shows that the distribution of colors at maximum and equivalent widths of blended Na I D1 and D2 narrow absorption features have a robust correlation with the Lira law $B-V$ decline rate, and that the division of the sample between fast and slow Lira law decliners by a Lira law $B-V$ decline rate of -0.013 (mag day^{-1}) is appropriate.

(A color version of this figure is available in the online journal.)

respectively, which is consistent with what has been found for highly reddened and normal SNe Ia (Folatelli et al. 2010; Mandel et al. 2011). At 55 days after maximum, we find that the reddening laws of fast and slow Lira law decliners are significantly different, but more similar to each other than at maximum light, with $R_V = 2.61 \pm 0.05$ and $R_V = 3.63 \pm 0.12$ for fast and slow Lira law $B-V$ decliners, respectively. These results are consistent with a contribution from light echoes and/or CSM dust destruction at late times, which would make the $B-V$ colors bluer. However, we cannot rule out an intrinsic relation between $V-i$ and $B-V$ colors at maximum light and at late times that could mimic some of our results, although this relation would need to be different for fast and slow Lira law $B-V$ decliners.

We have also studied the $V-i$ colors at maximum and 55 days after maximum of the SNe in the sample, in a similar fashion to $B-V$ colors. The probabilities that the distributions of $V-i$ colors at maximum light or 55 days after maximum of fast and slow Lira law $B-V$ decliners arise from the same parent population is 0.13 and 0.07, respectively. The lower significance obtained with these K-S tests may indicate that the effects we are measuring are stronger at bluer wavelengths.

3.4. Robustness and Systematic Errors

In the previous analysis, we set a seemingly arbitrary division of the sample at a Lira law $B-V$ decline rate, of -0.013 mag day^{-1}. In order to define this limiting decline rate, we performed a series of K-S tests for the distributions of EWs of blended Na I D1 and D2 narrow absorption and $B-V$ colors. The optimal division was defined by varying the dividing Lira law decline rate and finding small combined p values of the K-S tests for the distributions of EWs and $B-V$ colors, which corresponded to a dividing Lira law $B-V$ decline rate of about -0.013 mag day^{-1}. This is shown in Figure 6, where we also show the p values obtained for the K-S test associated with some of the environmental variables discussed before. This figure shows that (1) the equivalent width of blended Na I D1 and D2 narrow absorption features and the colors at maximum and 55 days after maximum have a minimum p value at a similar dividing Lira law decline rate and (2) the environmental variables considered in this analysis are never strongly associated with different Lira law decline rates, independently of the division of the sample used in the K-S tests. Comparing the range of Lira law decline rates considered with those found in Figure 2, we see that the high significance is not very sensitive to the dividing decline rate, making our conclusions more robust.

In order to check whether the results shown in the previous sections could be an artifact due to different measurement errors, we performed a K-S test on the distribution of the errors associated with the Lira law $B-V$ decline rate among the fast and slow Lira law $B-V$ decliners, obtaining no significant differences between them (p value $= 0.34$). In addition, in order to test whether our conclusions could be affected by constraining the sample to SNe with equivalent width errors lower than 0.6 Å and to SNe with Lira law $B-V$ decline rate errors lower than 0.006 mag day^{-1}, we relaxed both constraints, doubling the required errors, and obtained consistent results in all the relevant tests. Furthermore, to test whether fast and slow Lira law decliners are distributed differently with distance, which could affect some of our results through K corrections, we performed a K-S test on the distribution of the SN distances separating the sample between fast and slow decliners, obtaining no significant differences among the two groups (p value $=$ 0.49). To test this possible bias differently, we restricted our sample to SNe with a distance modulus smaller than 35 mag and repeated all the K-S tests from previous sections, obtaining consistent results again. Restricting the sample to only CfA3, CfA4, and CSP photometry, we also recover our main results, including different reddening laws between fast and slow Lira law $B-V$ decliners.

We have also repeated our K-S tests above after removing those SNe Ia that are known to be extreme cases of either high column densities, variable Na lines or peculiar ejecta properties: SN 2003cg, SN 2006X, SN 2007le, SN 2000cx and SN 2005hk, and our main conclusions remain the same. This indicates that the correlations found apply to a high fraction of SNe Ia, and not only to those SNe Ia which have strong CSM-like features like variable Na absorption.

Finally, in order to test whether the time interval used for measuring the Lira law $B-V$ decline rate (35–80 days after maximum) affects our conclusions, we have repeated the relevant tests using data from different time intervals after maximum. Later time photometry could have larger measurement errors and could therefore affect our best fitting decline rates. Also, the choice of the start of the Lira law regime is important since it could be too close to the observed peak in color evolution. Thus, we measured decline rates with the following time intervals after maximum: 30–90 days, 40–80 days, 30–70 days, and 50–90 days. In all but the last interval, between 50 and 90 days, we recover our main results. This could be due to the effect of larger errors or fewer data points at later times, or alternatively, to a systematic flattening of the decline rate at later times in the fast Lira law decliners.

3.5. Nebular Velocities

In FG12, a correlation between the presence of narrow absorption features and positive nebular velocity shifts (v_{neb}, introduced by Maeda et al. 2010) was found, which was interpreted as evidence for asymmetries in the CSM post explosion. In order to test whether the correlations found by

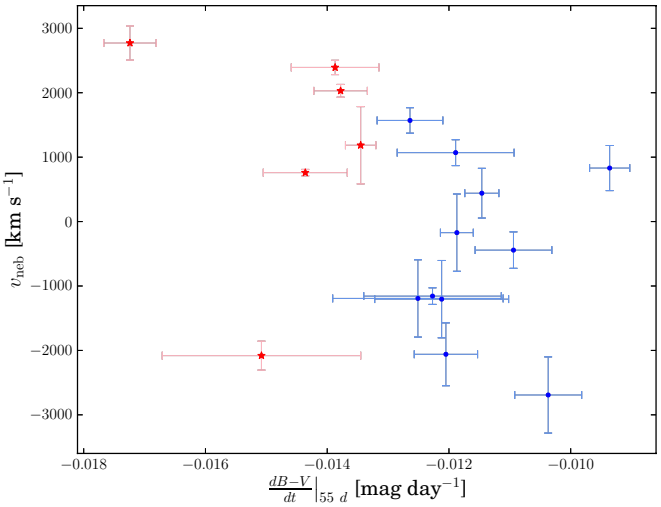

Figure 7. Nebular velocity shift of SNe Ia against their Lira law $B-V$ decline rate. Faster Lira law $B-V$ decliners appear to have positive nebular velocity shifts. The fast declining SN with $v_{\rm neb} < 0$ is SN 1994D (see discussion in the text).

(A color version of this figure is available in the online journal.)

FG12 are consistent with the results presented in this work, in Figure 7 we show the nebular velocity shift of nearby SNe Ia against their Lira law $B-V$ decline rate. For this we have taken a weighted average of the nebular velocities from Blondin et al. (2012) and Silverman et al. (2013). We could not reject the hypothesis that the distributions of nebular velocities of fast and slow Lira law $B-V$ decliners differ (p value of 0.09). Nonetheless, the number of SNe in the test is small, and by changing the definition interval for the Lira law $B-V$ decline rate from 35–80 days to 30–70 days, we obtain a p value of 0.003. This may suggest that SNe Ia with the fastest Lira law $B-V$ decline rates tend to have positive nebular velocity shifts. These are also the SNe found to have stronger Na I D1 and D2 absorption in FG12.

We note that in Figure 7, the fast declining SN with $v_{\rm neb} < 0$ is SN 1994D, which is the only SN in the sample whose Lira law $B-V$ decline rate differs significantly from the subtraction of its Lira law B and V decline rates, used in Figure 3. If the latter is used, then its decline rate becomes much lower, -0.011 ± 0.002 mag day^{-1} instead of -0.015 ± 0.001, a difference which is explained by non-simultaneous B and V photometry for some days, which cannot be used to measure $B-V$ decline rates directly. If this different value is used, then we obtain a p value of 0.02 for the probability that the distributions of nebular velocities of fast and slow Lira law $B-V$ decliners arise from the same population.

Given the correlation found by Maeda et al. (2010) between nebular velocities and broad Si II λ6355 absorption velocity gradients, we investigated whether the Lira law $B-V$ decline rates are related to the Si II absorption velocity at maximum. We measured the Si II velocities at different epochs and obtained values at maximum by interpolation, then combined these values with measurements from other sources (Benetti et al. 2005; Foley et al. 2011; Silverman et al. 2012; G. Folatelli et al. 2013, in preparation), using weights inversely proportional to the errors to obtain averages. We tested whether Si II absorption velocities at maximum are related to Lira law $B-V$ decline rates, colors at maximum (as found by Wang et al. 2009 and Foley et al. 2011), or EWs of blended Na narrow absorption features, which would be consistent with the excess blueshift found by Foley et al. (2012). We found that there is a probability of 0.07 that the distributions of Lira law $B-V$ decline rates of SNe Ia with Si II velocities faster or slower than 11,800 (km s^{-1}) arise from the same parent population, a probability of 0.002 that the distributions of colors at maximum of fast and slow Si II velocity SNe Ia arise from the same parent population, a probability of 0.81 that the distributions of EWs of narrow Na absorption of fast and slow Si II velocity SNe Ia arise from the same parent population, and a probability of 0.07 that the distributions of morphological types of fast and slow Si II velocity SNe Ia arise from the same parent population. This confirms the color differences found by Wang et al. (2009) and suggests a further connection with Lira law $B-V$ decline rates. The non-detection of significant differences in the distribution of EWs of Na absorption or morphological type with Si II velocity may indicate that some of these color differences are intrinsic, or that our sample size is not large enough, given the recent finding by Wang et al. (2013) of different radial distributions for fast and slow Si II velocity SNe Ia.

3.6. ISM as the Origin of Lira Law Decline Rate Variations?

Although the previous tests suggest that environmental factors do not contribute to the Lira law $B-V$ decline rate, it is intriguing that in Figure 6 the region where the p values associated with tests for a relation between Lira law decline rates and the host galaxy morphological type or inclination are lowest coincides with the region where p values associated with EWs or colors are also the lowest. This led us to consider whether the ISM could really affect the Lira law $B-V$ decline rate in some way.

Since the inclination of a galaxy should not be related to the presence or absence of CSM in SNe Ia, and given that the ISM will generally be too distant from the SN explosion to produce significant light echoes or to be destroyed by the expanding ejecta between 35 and 80 days after maximum, a different mechanism to produce changes in the Lira law $B-V$ decline rate would be needed. Note that we are not referring to ISM light echoes (Wang et al. 2008a), which can affect the light curves at even later times than those considered in this work. In fact, the transversal expansion of the ejecta in an inhomogeneous distribution of projected column densities of the host galaxy ISM could affect the Lira law $B-V$ decline rate by changing the average column density as the photospheric radius increases. If this is the case, then what needs to be shown is whether systems that have stronger Na I D1 and D2 absorption and redder colors at maximum are also expected to have faster Lira law $B-V$ decline rates due to this effect.

For this, we follow the approach of Patat et al. (2010) to study the effect of the transversal expansion of the ejecta in a non-homogeneous ISM. Assuming their approximation for the evolution of the SN photospheric radius with time, and using random realizations of the ISM column density assuming a fractal structure with a power law of -2.75 on spatial scales down to the size of the photosphere, we compute the average column density within the photospheric radius as the SN expands. In the left panel of Figure 8, we show one realization of the dust column density with different photospheric radii shown as the SN expands. In this example, because the SN started behind a relatively overdense region, the average column density started at a relatively large value and tended to decrease with time due to a dilution effect as the photospheric radius increases. In the right panel of Figure 8, we show the expected

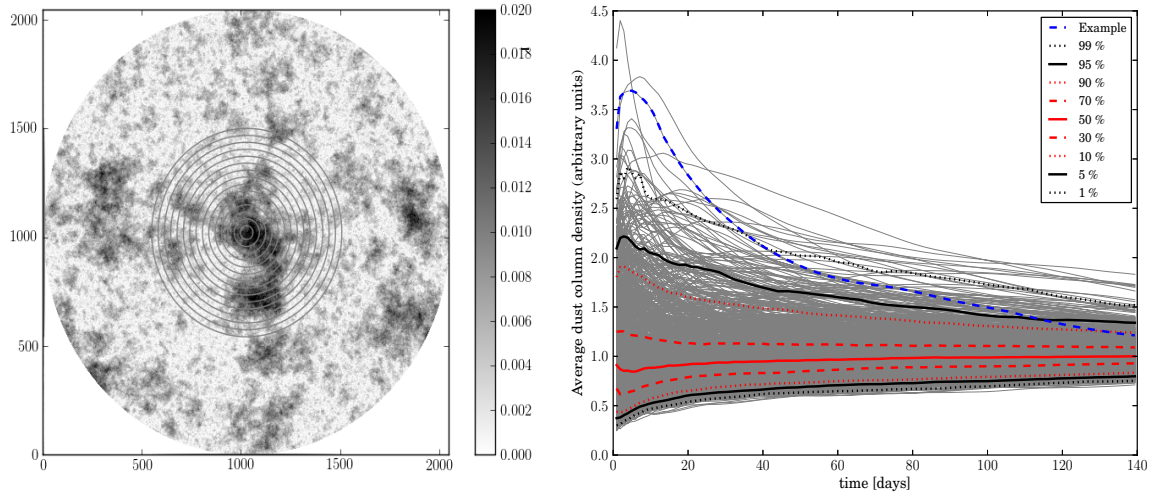

Figure 8. Left: example dust realization from the observer's perspective following the procedure of Patat et al. (2010) compared to the typical size of the SN Ia photosphere up to 100 days after explosion. Right: evolution of the average column density within the photospheric disc of SNe Ia in 1000 ISM realizations. Most of the dust column density variations are found at earlier times. This means that the most reddened objects at earlier times will be less reddened at later times, implying a faster Lira law $B-V$ decline rate. The dashed-blue line corresponds to the example ISM realization shown, which is very atypical among the simulated ISM realizations.

(A color version of this figure is available in the online journal.)

evolution of the average column density for one thousand ISM realizations, showing different percentiles for reference. This figure shows that the biggest dispersion occurs at early times, when chance alignments with under- or overdense regions can dominate, but the dilution effect occurring at later times will make the dispersion of the average column densities decrease.

Thus, Figure 8 shows that the inhomogeneous nature of the ISM will naturally produce SNe Ia that have stronger EWs of narrow blended Na I D1 and D2 absorption and are redder at maximum, and that have fast-evolving average column densities, and therefore faster Lira law $B-V$ decline rates. The higher the inclination, the stronger the effect, as the typical column density will tend to increase. Moreover, at later times, the colors will be dominated by the overall column density, which could explain why SNe Ia in later morphological types are significantly redder at later times. However, this effect would not explain the differences in reddening laws observed between fast and slow Lira law $B-V$ decliners.

Nonetheless, the column density is expected to be proportional to the product of the color excess and R_V, and a detailed analysis of Figure 8 implies that at maximum light the $B-V$ colors of the SNe in the percentiles 50 and 95 should differ by about 0.25 mag,[7] or by about 0.12 mag for the percentiles 30 and 70. At 55 days after maximum, the $B-V$ colors of the SNe in the percentiles 50 and 95 should differ by about 0.15 mag, and by about 0.08 for the percentiles 30 and 70. These magnitude differences are of the same order as those seen in Figure 1, but are not consistent with the lack of correlation between the Lira law V-band and $B-V$ decline rates observed in Figure 3(b). This suggests that the inhomogeneous nature of the ISM can not explain all our findings, and that a more detailed analysis will be needed to exclude this possibility.

4. DISCUSSION AND CONCLUSIONS

In this work, we have shown that there are significant differences in the $B-V$ evolution of SNe Ia during the Lira law regime, between 35 and 80 days after maximum. These differences are driven by the evolution of SNe Ia in the B band: fast Lira law $B-V$ decliners are slow Lira law B decliners. With the sample defined in Section 2, we have shown that fast Lira law $B-V$ decliners, defined as having Lira law $B-V$ decline rates smaller than -0.013 mag day^{-1}, have stronger narrow absorption lines of blended Na I D1 and D2, are redder, and have a lower R_V extinction law at maximum light and 55 days after maximum light. The differences in colors were stronger at maximum light.

Additionally, we did not find a highly significant difference between the distributions of host galaxy morphological type, host galaxy inclination, stretch, or Δm_{15} dividing the sample by Lira law $B-V$ decline rate. This suggests that the Lira law $B-V$ decline rates are not strongly dependent on the age of the SN Ia progenitor systems, are not strongly affected by ISM, and are not mainly driven by the mass of nickel in the ejecta, the main parameter of SN Ia light curves.

For the sample of 89 SNe Ia that had good photometric coverage up to late times, we found that their colors at maximum were consistent between earlier- and later-type galaxies. The colors 55 days after maximum were significantly different between earlier- and later-type galaxies, suggesting that the extinction at later times is more clearly connected to ISM and that late time colors may be a better proxy for environment. If CSM is dominant at early times, then the canceling effect on the color excess due to CSM light echoes or to dust destruction as the ejecta sweeps over the CSM could explain this result.

An SN explosion surrounded by CSM should sublimate dust and ionize Na I up to some maximum radii, therefore the CSM should have a characteristic minimum radius, r_{CSM}, which is thought to be between 0.01 and 0.1 pc for Na I (Patat et al. 2007; Simon et al. 2009), and which is expected to be of the same order of magnitude for dust (Amanullah & Goobar 2011). Photons leaving the ejecta at maximum light could be seen as light echoes 55 days after maximum if they are reflected after traveling for about 55 days, or a typical distance of about 0.05 pc, which is of the order of this minimum CSM radius. However, light echoes are not the only mechanism that can produce this

[7] $-2.5\log(n_{95}/n_{50})/R_V = -0.25$ assuming $R_V = 3.2$, $n_{95} = 1.9$ units and $n_{50} = 0.9$ units.

effect: depending on the outer ejecta speed, which we assume to be one tenth of the speed of light, the ejecta could have traveled up to about 0.001 pc at maximum light; therefore, it should not have time to interact with the CSM and sublimate CSM dust. However, 55 days after maximum light, the ejecta could be approaching the inner edge of the CSM, since it will have traveled up to about 0.006 pc, and it could start reducing the dust column density. This could explain why the differences in colors and extinction laws found at maximum light between fast and slow Lira law decliners were not as strong 55 days after maximum, but also why environmental effects explain some of the differences in colors 55 days after maximum.

It is interesting to note that smaller dust sublimation or Na I D1 and D2 ionization CSM radii should produce more extinction and stronger narrow absorption features, which we find in fast Lira law $B-V$ declining SNe Ia. For the same ejection velocity and mass loss rate before an SN explosion, the dust column density and extinction should scale as $r_{\rm CSM}^{-2}$. Smaller CSM dust inner radii should also produce stronger CSM light echoes, since their intensity should scale as $r_{\rm CSM}^{-4}$, which would be reflected in faster $B-V$ evolution at late times because of the slower expected Lira law B-band decline rates. In fact, Amanullah & Goobar (2011) showed that smaller CSM radii should affect more significantly the $B-V$ evolution at later times, producing faster Lira law $B-V$ decline rates.

The resulting fast declining sample is composed of 29 SNe Ia (33%), and the slow declining sample of 60 SNe Ia (67%). Interestingly, the fraction of fast Lira decliners is similar to the fraction of 35% high velocity SNe Ia (HV SNe Ia, with $v({\rm Si\ II})_{\rm max} \geqslant 11{,}800$ (km s^{-1})) among the group of normal SNe Ia found by Wang et al. (2009), or the excess of about 25% of SNe Ia with blueshifted absorption features detected by Sternberg et al. (2011), which is also consistent with the excess of blueshifted systems among HV SNe Ia found by Foley et al. (2012). This suggests that blueshifted narrow absorption features, high velocity Si II features at maximum, high EWs of narrow absorption features, redder colors at maximum, fast Lira law decline rates, and lower R_V reddening laws may all be associated with the same population, which in our interpretation is the one with significant CSM. Unfortunately, there is no overlap between our sample and the recent sample of CSM-interacting SNe Ia found by Silverman et al. (2013). The overlap between our sample and that from Sternberg et al. (2011) is very small (only 4 SNe) and we cannot test whether their blueshifted sample corresponds to our fast declining sample. However, the two overlapping SNe Ia in their blueshifted sample are also fast Lira law $B-V$ decliners in our sample, SN 2006X and SN 2007le, and they also happen to have variable Na I D1 and D2 narrow absorption features (Patat et al. 2007; Simon et al. 2009), which is expected in the CSM interpretation.

In the context of FG12, we have found a weak correlation between nebular velocity shifts ($v_{\rm neb}$) and Lira law $B-V$ decline rates, which is consistent with the interpretation of FG12, but which needs to be confirmed with a bigger sample.[8] This would mean that SNe Ia with $v_{\rm neb} \geqslant 0$ have stronger EWs of Na I D1 and D2, are redder at maximum light, have faster Lira law $B-V$ decline rates, and have lower R_V reddening laws at maximum light because they have more CSM in their line of sight. Assuming that about 33% of the SNe Ia have significant CSM in the line sight and that $v_{\rm neb}$ is a good proxy for explosion viewing angle, this would mean that there is a comparable population of SNe Ia with negative nebular velocities that would also have significant CSM, but which we do not see in narrow absorption features or fast Lira law $B-V$ decline rates because their CSM is on the opposite side of their ejecta. Here it should be noted that dust scattering is primarily forward scattering (Henyey & Greenstein 1941), which means that light echoes would be best seen when the CSM is between the SNe and the observer ($v_{\rm neb} \geqslant 0$ in FG12). Although the fractions are uncertain at the moment, this leaves room for additional progenitor scenarios that do not fit in this CSM picture.

Since changes in the Lira law decline rate could be easily produced by CSM (Amanullah & Goobar 2011, see their Figure 8), and given that we did not find any significant environmental dependency of the Lira law $B-V$ decline rates, we propose that the differences found between fast and slow Lira law $B-V$ decliners are due to CSM, but we also investigate the possibility that a similar result could be produced by ISM. We showed that the transversal expansion of the SN photosphere within an inhomogeneous distribution of column densities could naturally lead to faster Lira law decliners having stronger absorption at maximum as discussed in Section 3.6, but further modeling is required to exclude this possibility, or a significant contribution of ISM light echoes at early times (e.g., Patat 2005; Patat et al. 2006).

This work is an addition to the growing evidence for CSM in SNe Ia, but we believe that only the use of high resolution spectra (Sternberg et al. 2011; Foley et al. 2012) will help better constrain the nature of the absorbing material in SNe Ia. The lack of evidence for shocked winds, shocked companion stars, companion stars in pre-supernova images, or companion stars in SN Ia remnants (e.g., Li et al. 2011; Nugent et al. 2011; Bloom et al. 2012; Brown et al. 2012; Schaefer & Pagnotta 2012; Edwards et al. 2012) may indicate that the progenitors of SNe Ia arise from more than one progenitor scenario or from more complicated scenarios that we have not yet imagined.

Finally, although it is still possible that the physics of positron absorption could be responsible for the variations of the Lira law detected, this effect should depend on the age of the progenitors in order to produce stronger narrow absorption features due to larger ISM column densities. The fact that we do not find a strong dependency between Lira law decline rates and environment, stretch, or Δm_{15} suggests that this is not the case. Additional studies of the relation between very late $B-V$ decline rates (e.g., beyond 200 days) and the Lira law $B-V$ decline rate could be used to provide a clean separation between the effects of CSM and the physics of positron absorption (see, e.g., Lair et al. 2006).

We thank an anonymous referee for useful suggestions that improved the quality of the manuscript. We also thank M. Phillips, G. Pignata, M. Hamuy, J. Anderson, F. Bufano, P. Zelaya, A. Clochiatti, J. Faherty, and P. Román for many useful discussions. F.F. and S.G. acknowledge support from FONDECYT through grants 3110042 and 3130680, respectively. F.F and S.G. acknowledge support provided by the Millennium Center for Supernova Science through grant P10-064-F (funded by "Programa Bicentenario de Ciencia y Tecnología de CONICYT" and "Programa Iniciativa Científica Milenio de MIDEPLAN"). F.F. acknowledges partial support from Comité Mixto ESO-GOBIERNO DE CHILE. G.F. acknowledges support from the World Premier International Research Center Initiative (WPI Initiative), MEXT, Japan, and

[8] We have confirmed the correlation between narrow absorption Na lines and nebular velocities using the public spectra from Silverman et al. (2013) and the method described in FG12.

from Grant-in-Aid for Scientific Research for Young Scientists (23740175). This research has made use of the CfA Supernova Archive, which is funded in part by the National Science Foundation through grant AST 0907903.

REFERENCES

Altavilla, G., Fiorentino, G., Marconi, M., et al. 2004, MNRAS, 349, 1344
Amanullah, R., & Goobar, A. 2011, ApJ, 735, 20
Anupama, G. C., Sahu, D. K., & Jose, J. 2005, A&A, 429, 667
Barbon, R., Buondí, V., Cappellaro, E., & Turatto, M. 1999, A&AS, 139, 531
Benetti, S., Cappellaro, E., Mazzali, P. A., et al. 2005, ApJ, 623, 1011
Benetti, S., Meikle, P., Stehle, M., et al. 2004, MNRAS, 348, 261
Blondin, S., Matheson, T., Kirshner, R. P., et al. 2012, AJ, 143, 126
Blondin, S., Prieto, J. L., Patat, F., et al. 2009, ApJ, 693, 207
Bloom, J. S., Kasen, D., Shen, K. J., et al. 2012, ApJL, 744, L17
Brown, P. J., Dawson, K. S., de Pasquale, M., et al. 2012, ApJ, 753, 22
Burns, C. R., Stritzinger, M., Phillips, M. M., et al. 2011, AJ, 141, 19
Candia, P., Krisciunas, K., Suntzeff, N. B., et al. 2003, PASP, 115, 277
Cappellaro, E., Mazzali, P. A., Benetti, S., et al. 1997, A&A, 328, 203
Cardelli, J. A., Clayton, G. C., & Mathis, J. S. 1989, ApJ, 345, 245
Chevalier, R. A. 1986, ApJ, 308, 225
Conley, A., Sullivan, M., Hsiao, E. Y., et al. 2008, ApJ, 681, 482
Contreras, C., Hamuy, M., Phillips, M. M., et al. 2010, AJ, 139, 519
Dilday, B., Howell, D. A., Cenko, S. B., et al. 2012, Sci, 337, 942
Edwards, Z. I., Pagnotta, A., & Schaefer, B. E. 2012, ApJL, 747, L19
Elias-Rosa, N., Benetti, S., Cappellaro, E., et al. 2006, MNRAS, 369, 1880
Folatelli, G., Morrell, N., Phillips, M. M., et al. 2013, ApJ, in press (arXiv:1305.6997)
Folatelli, G., Phillips, M. M., Burns, C. R., et al. 2010, AJ, 139, 120
Foley, R. J., Sanders, N. E., & Kirshner, R. P. 2011, ApJ, 742, 89
Foley, R. J., Simon, J. D., Burns, C. R., et al. 2012, ApJ, 752, 101
Förster, F., González-Gaitán, S., Anderson, J., et al. 2012, ApJL, 754, L21
Fryer, C. L., Ruiter, A. J., Belczynski, K., et al. 2010, ApJ, 725, 296
Ganeshalingam, M., Li, W., Filippenko, A. V., et al. 2010, ApJS, 190, 418
Gerardy, C. L., Meikle, W. P. S., Kotak, R., et al. 2007, ApJ, 661, 995
Goobar, A. 2008, ApJL, 686, L103
Hachisu, I., Kato, M., & Nomoto, K. 1996, ApJL, 470, L97
Hachisu, I., Kato, M., & Nomoto, K. 1999a, ApJ, 522, 487
Hachisu, I., Kato, M., Nomoto, K., & Umeda, H. 1999b, ApJ, 519, 314
Hamuy, M., Phillips, M. M., Maza, J., et al. 1995, AJ, 109, 1
Hamuy, M., Phillips, M. M., Suntzeff, N. B., et al. 1996, AJ, 112, 2398
Hamuy, M., Phillips, M. M., Suntzeff, N. B., et al. 1996, AJ, 112, 2408
Hamuy, M., Trager, S. C., Pinto, P. A., et al. 2000, AJ, 120, 1479
Han, Z., & Podsiadlowski, P. 2004, MNRAS, 350, 1301
Henyey, L. G., & Greenstein, J. L. 1941, ApJ, 93, 70
Hicken, M., Challis, P., Jha, S., et al. 2009, ApJ, 700, 331
Hicken, M., Challis, P., Kirshner, R. P., et al. 2012, ApJS, 200, 12
Hillebrandt, W., & Niemeyer, J. C. 2000, ARA&A, 38, 191
Horesh, A., Kulkarni, S. R., Fox, D. B., et al. 2012, ApJ, 746, 21
Hsiao, E. Y., Conley, A., Howell, D. A., et al. 2007, ApJ, 663, 1187
Iben, I., Jr., & Tutukov, A. V. 1984, ApJS, 54, 335
Jha, S., Kirshner, R. P., Challis, P., et al. 2006, AJ, 131, 527
Johansson, J., Thomas, D., Pforr, J., et al. 2013, MNRAS, 431, 43
Khokhlov, A. M. 1991, A&A, 245, L25
Kobayashi, C., & Nomoto, K. 2009, ApJ, 707, 1466
Krisciunas, K., Hastings, N. C., Loomis, K., et al. 2000, ApJ, 539, 658
Krisciunas, K., Phillips, M. M., Stubbs, C., et al. 2001, AJ, 122, 1616
Krisciunas, K., Suntzeff, N. B., Candia, P., et al. 2003, AJ, 125, 166
Krisciunas, K., Suntzeff, N. B., Phillips, M. M., et al. 2004, AJ, 128, 3034
Kromer, M., Fink, M., Stanishev, V., et al. 2013, MNRAS, 429, 2287
Kromer, M., Sim, S. A., Fink, M., et al. 2010, ApJ, 719, 1067
Lair, J. C., Leising, M. D., Milne, P. A., & Williams, G. G. 2006, AJ, 132, 2024
Landolt, A. U. 1992, AJ, 104, 372
Langer, N., Deutschmann, A., Wellstein, S., & Höflich, P. 2000, A&A, 362, 1046
Leonard, D. C., Li, W., Filippenko, A. V., Foley, R. J., & Chornock, R. 2005, ApJ, 632, 450
Li, W., Bloom, J. S., Podsiadlowski, P., et al. 2011, Natur, 480, 348
Li, X.-D., & van den Heuvel, E. P. J. 1997, A&A, 322, L9
Lira, P. 1995, Masters Thesis, Universidad de Chile
Maeda, K., Benetti, S., Stritzinger, M., et al. 2010, Natur, 466, 82
Maeda, K., Taubenberger, S., Sollerman, J., et al. 2010, ApJ, 708, 1703
Mandel, K. S., Narayan, G., & Kirshner, R. P. 2011, ApJ, 731, 120
Maoz, D., & Mannucci, F. 2012, PASA, 29, 447
Matteucci, F., & Greggio, L. 1986, A&A, 154, 279
Meikle, W. P. S., Cumming, R. J., Geballe, T. R., et al. 1996, MNRAS, 281, 263
Meng, X., Chen, X., & Han, Z. 2009, MNRAS, 395, 2103
Milne, P. A., The, L.-S., & Leising, M. D. 1999, ApJS, 124, 503
Nomoto, K. 1982, ApJ, 257, 780
Nomoto, K., Thielemann, F.-K., & Yokoi, K. 1984, ApJ, 286, 644
Nugent, P. E., Sullivan, M., Cenko, S. B., et al. 2011, Natur, 480, 344
O'Donnell, J. E. 1994, ApJ, 422, 158
Pakmor, R., Kromer, M., Taubenberger, S., et al. 2012, ApJL, 747, L10
Patat, F. 2005, MNRAS, 357, 1161
Patat, F., Benetti, S., Cappellaro, E., & Turatto, M. 2006, MNRAS, 369, 1949
Patat, F., Chandra, P., Chevalier, R., et al. 2007, Sci, 317, 924
Patat, F., Cox, N. L. J., Parrent, J., & Branch, D. 2010, A&A, 514, A78
Perlmutter, S., Aldering, G., Goldhaber, G., et al. 1999, ApJ, 517, 565
Phillips, M. M. 1993, ApJL, 413, L105
Phillips, M. M., Krisciunas, K., Suntzeff, N. B., et al. 2006, AJ, 131, 2615
Phillips, M. M., Lira, P., Suntzeff, N. B., et al. 1999, AJ, 118, 1766
Riess, A. G., Filippenko, A. V., Challis, P., et al. 1998, AJ, 116, 1009
Riess, A. G., Kirshner, R. P., Schmidt, B. P., et al. 1999, AJ, 117, 707
Riess, A. G., Li, W., Stetson, P. B., et al. 2005, ApJ, 627, 579
Röpke, F. K., Kromer, M., Seitenzahl, I. R., et al. 2012, ApJL, 750, L19
Röpke, F. K., & Niemeyer, J. C. 2007, A&A, 464, 683
Sadakane, K., Yokoo, T., Arimoto, J.-I., et al. 1996, PASJ, 48, 51
Schaefer, B. E., & Pagnotta, A. 2012, Natur, 481, 164
Schlegel, D. J., Finkbeiner, D. P., & Davis, M. 1998, ApJ, 500, 525
Silverman, J. M., Foley, R. J., Filippenko, A. V., et al. 2012, MNRAS, 425, 1789
Silverman, J. M., Ganeshalingam, M., & Filippenko, A. V. 2013, MNRAS, 430, 1030
Silverman, J. M., Nugent, P. E., Gal-Yam, A., et al. 2013, arXiv:1304.0763
Sim, S. A., Röpke, F. K., Hillebrandt, W., et al. 2010, ApJL, 714, L52
Simon, J. D., Gal-Yam, A., Gnat, O., et al. 2009, ApJ, 702, 1157
Sollerman, J., Lindahl, J., Kozma, C., et al. 2004, A&A, 428, 555
Stanishev, V., Goobar, A., Benetti, S., et al. 2007, A&A, 469, 645
Sternberg, A., Gal-Yam, A., Simon, J. D., et al. 2011, Sci, 333, 856
Stritzinger, M., Burns, C. R., Phillips, M. M., et al. 2010, AJ, 140, 2036
Stritzinger, M. D., Phillips, M. M., Boldt, L. N., et al. 2011, AJ, 142, 156
Sullivan, M., Conley, A., Howell, D. A., et al. 2010, MNRAS, 406, 782
Sullivan, M., Le Borgne, D., Pritchet, C. J., et al. 2006, ApJ, 648, 868
Wang, B., Chen, X., Meng, X., & Han, Z. 2009, ApJ, 701, 1540
Wang, B., & Han, Z. 2012, NewAR, 56, 122
Wang, L. 2005, ApJL, 635, L33
Wang, X., Filippenko, A. V., Ganeshalingam, M., et al. 2009, ApJL, 699, L139
Wang, X., Li, W., Filippenko, A. V., et al. 2008a, ApJ, 677, 1060
Wang, X., Li, W., Filippenko, A. V., et al. 2008b, ApJ, 675, 626
Wang, X., Wang, L., Filippenko, A. V., Zhang, T., & Zhao, X. 2013, Sci, 340, 170
Webbink, R. F. 1984, ApJ, 277, 355
Woosley, S. E., Taam, R. E., & Weaver, T. A. 1986, ApJ, 301, 601